Reconstruction of the GaAs (311) *A* surface

M. Wassermeier
Paul-Drude-Institute für Festkörperelektronik, Hausvogteiplatz 5-7, 10117 Berlin, Germany

J. Sudijono,* M. D. Johnson, K. T. Leung, and B. G. Orr
The Harrison M. Randall Laboratory, University of Michigan, Ann Arbor, Michigan 48109-1120

L. Däweritz and K. Ploog
Paul-Drude-Institute für Festkörperelektronik, Hausvogteiplatz 5-7, 10117 Berlin, Germany
(Received 14 February 1995)

We study the reconstruction of the GaAs (311) *A* surface with reflection high-energy electron-diffraction (RHEED) and scanning tunneling microscopy (STM). The surface observed *in situ* with RHEED during molecular-beam epitaxy is distinguished by a lateral periodicity of 3.2 nm perpendicular to the [$\bar{2}33$] direction. This periodicity is confirmed employing *in situ* STM. High-resolution STM images furthermore reveal a surface reconstruction characterized by a dimerization of the surface As atoms. We show how the reconstruction can be formed, applying a simple electron-counting model. The excellent agreement with the experimental results further support this model, which was already found to explain the reconstructions of the (100) and the (111) surfaces. In order to form a semiconducting surface, the three uppermost layers are involved in the reconstruction process, giving rise to a depth modulation of 0.34 nm.

Molecular-beam epitaxy (MBE) of III-V semiconductors on different surface orientations has recently attracted much interest in the quest for new growth modes as candidates for the direct synthesis of quantum wires and quantum dots.[1] On unpatterned substrates, lateral confinement of free carriers to dimensions below their Fermi wavelength has so far been exploited successfully for devices only for the case of one dimension, namely, for quantum-well lasers. In order to extend this concept to two or even all three spatial dimensions, different growth techniques have been tried and proposed.[2] Recently, Nötzel *et al.*,[3] reported the formation of quantum wires during the growth of GaAs/AlAs superlattices on the GaAs (311) *A* surface. This surface was anticipated to spontaneously form a corrugation, with a lateral 3.2-nm periodicity and a step height of 6 ML (1.02 nm), due to the formation of {331} facets. In this Brief Report, we present high-resolution scanning-tunneling-microscopy (STM) images of the (311) *A* surface. The lateral periodicity of the reconstructed surface is found to be the same as previously reported, whereas the step height is only 2 ML (0.34 nm) and, thus, substantially smaller than extracted from the high-energy electron-diffraction (RHEED) study of Nötzel *et al.*[3] The reconstruction can, in fact, be predicted by a model that has successfully explained also the reconstructions on other GaAs surface orientations.

The GaAs surfaces that have been studied so far by STM are the (100) surface,[4] the (110) surface,[5] and the (111)*B* surface.[6] Only the (110) surface is nonpolar and, with respect to the ideal, i.e., unreconstructed surface, merely a relaxation has been found to take place on this surface.[7] The polar (100) and (111) surfaces, however, undergo a substantial surface reconstruction to lower their surface energies. The driving force for this process has been outlined by Harrison.[8] His work forms the basis of most of the calculations on the different GaAs surfaces, and can be expressed in a very simple model. This electron-counting model formulates a recipe to form the surface reconstruction and successfully describes all of the semiconducting surface reconstructions found so far on the (100) and the (111) surfaces of GaAs. It demands that the surface reconstructs in such a way, that all the As dangling bonds are filled and the Ga dangling bonds are emptied. This notion also agrees with the results of total-energy calculations that have been performed on the (100) surface[9] and the (111) surface.[10,11]

Surface-energy calculations also exist for the (311) *A* surface.[12] In this work, an As dimerization is expected to increase the stability of the surface significantly.

The experiments have been performed in a combined MBE-STM chamber described elsewhere.[13] After thermal oxide desorption at a temperature of 630 °C measured with a pyrometer facing the sample, the temperature is lowered to 580 °C. An As_4 background pressure of 3.8×10^{-6} Torr measured with an ion gauge close to the sample position was used during the growth. The RHEED pattern, measured at an electron energy of 10 keV, shows a (1×1) symmetry at this point. After the growth of the first 2 nm at a growth rate of 0.1 μm/h, the characteristic diffraction streaks along the [$\bar{2}33$] direction with a reciprocal lattice rod spacing of $\frac{1}{16}$ of the spacing to the first-order bulk diffraction spot appear. In general, we find that the optimum growth conditions on this surface are very similar to those on the (100) surface. After the growth of 20 nm, the complete set of diffraction streaks from the specular beam to the first-order bulk diffraction spot is observed as shown in Fig. 1. The first-order bulk diffraction spot ($a^{-1}=5$ nm^{-1}) shows up from behind the shadow edge at the 16th diffraction streak

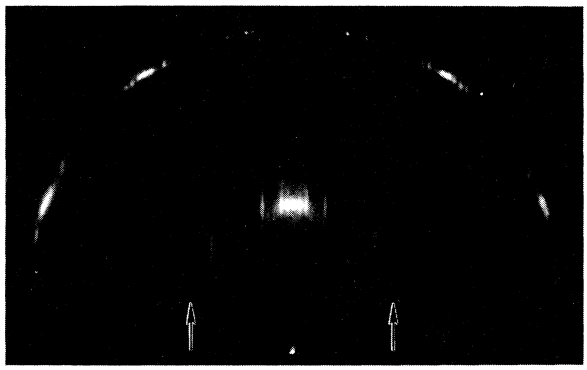

FIG. 1. RHEED pattern taken along the [$\bar{2}33$] direction with a 10-keV electron-beam energy. The position of the first-order bulk diffraction spots is indicated by the arrows.

(marked with an arrow in Fig. 1). A lateral periodicity of 3.2 nm perpendicular to the [$\bar{2}33$] direction can thus be deduced.[3] The RHEED pattern differs, however, from that previously reported[3] in that no clear splitting along the streaks was observed, although at incident polar angles below 0.9° the intensity distribution becomes similar. It can, therefore, not be excluded that there are differences in the structures or the RHEED diffraction conditions in this and the previous work. The previously proposed model describes the corrugated surface as composed of narrow (311) terraces and two sets of {331} facets. In the interpretation of the RHEED pattern, it has been assumed that the surface corrugation can be approximated by a two-level system of alternating upward downward steps of 1.02 nm height.[14] It cannot be excluded that the pronounced splitting observed in Refs. 3 and 14 might also be due to the slight miscut of the samples used in their investigation.

The quenching of the surface reconstruction is achieved in two steps. First the substrate temperature is lowered to 450 °C while the As source cools down to room temperature. After the background pressure in the MBE chamber has fallen below 2×10^{-10} Torr, the substrate temperature is lowered to room temperature, and the sample is transferred to the STM chamber and mounted on the STM sample post. We point out that, as judged by eyes, the RHEED pattern does not change during the quenching process nor after the STM imaging. Thus, we assume that the surface reconstruction remains unchanged.

Figure 2(a) shows a STM filled-state image of a 200×200 nm^2 area of the surface. A constant tunneling current of 40 pA at a tip voltage of +2.94 V was used for this image. We find rows running along the [$\bar{2}33$] direction with a lateral spacing of 3.2 nm as expected from the RHEED pattern. Linescans reveal a ML height of 0.17 ± 0.02 nm. The highly anisotropic surface roughness of 5 ML is typical for this surface. Filled- and empty-state STM images look the same on this surface, which is similar to the finding on the (100) surface and can be attributed to the similarity of the topographic and the density-of-state contribution to the tunneling current.[15]

A high-resolution 16×16 nm^2 large STM empty-state image, collected at a tip-voltage of −2.65 V and a tunneling current of 65 pA, is shown in Fig. 2(b). In this image we also observe a corrugation along and between the rows shown in the large scan image of Fig. 2(a). The higher resolution discloses a surface reconstruction, involving the three uppermost layers. Between the two rows of the first layer zigzagging along the [$\bar{2}33$] direction, we find two similar rows 1 ML (0.17 nm) below the first, whose periodic corrugation along the [$\bar{2}33$] direction is phase shifted with respect to the uppermost rows by 0.6 ± 0.1 nm. The trench between the rows in this second layer opens a window to the third layer. The lateral distance between the rows in the second-layer mea-

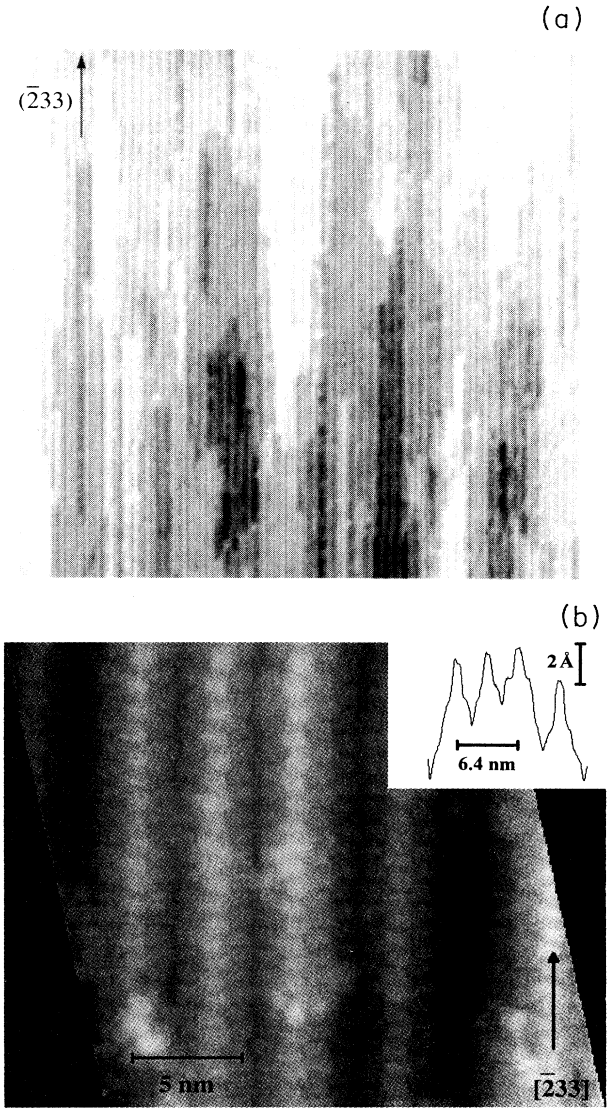

FIG. 2. STM images of the reconstructed (311)A surface. (a) A 200×200 nm^2 larger filled-state image showing the 3.2-nm periodicity perpendicular to the [$\bar{2}33$] direction. The surface exhibits a mesoscopic scale roughness of up to 5 ML. (b) A high-resolution empty-state image revealing the atomic structure of the reconstruction that involves the three uppermost surface layers. The linescan in the inset reveals a height modulation of the reconstruction within the same atomic layer of 0.3 ± 0.5 nm.

sures 1.2 ± 0.2 nm and is larger than the distance measured between the second-layer row and the first-layer row, which is measured to be 1.0 ± 0.1 nm. The inset in Fig. 2(b) shows a linescan of the STM image along the $[0\bar{1}1]$ direction. It includes the three As dimer rows of the uppermost atomic layer as well as the step to the next layer and one As dimer row in this layer. The linescan reveals a height modulation within the same atomic layer of 0.3 ± 0.05 nm, which correspond to two atomic layers. This is substantially smaller than the corrugation proposed in Refs. 3 and 14.

With the help of the high-resolution STM images and the electron-counting model, the surface reconstruction can be identified. The $(311)A$ surface, shown in Fig. 3(a), results by tilting the surface plane from the (100) surface towards the $(111)A$ surface by 25.2°. It can thus be viewed as a hybrid of the two surfaces, which manifests itself also in the atomic structure of the ideal surface: The surface atomic layer contains both As and Ga atoms to the same amount. The layer of the twofold-coordinated (100)-like As atoms is 0.043 nm above the layer of the threefold-coordinated $(111)A$-like Ga atoms. For the surface reconstruction, a (100)-like dimerization can be constructed in accordance with the electron-counting model as will be shown below. The unit cell of the ideal surface is 0.4×1.35 nm^2 large. Adjacent units cells in the $[\bar{2}33]$ direction are shifted by half a unit cell

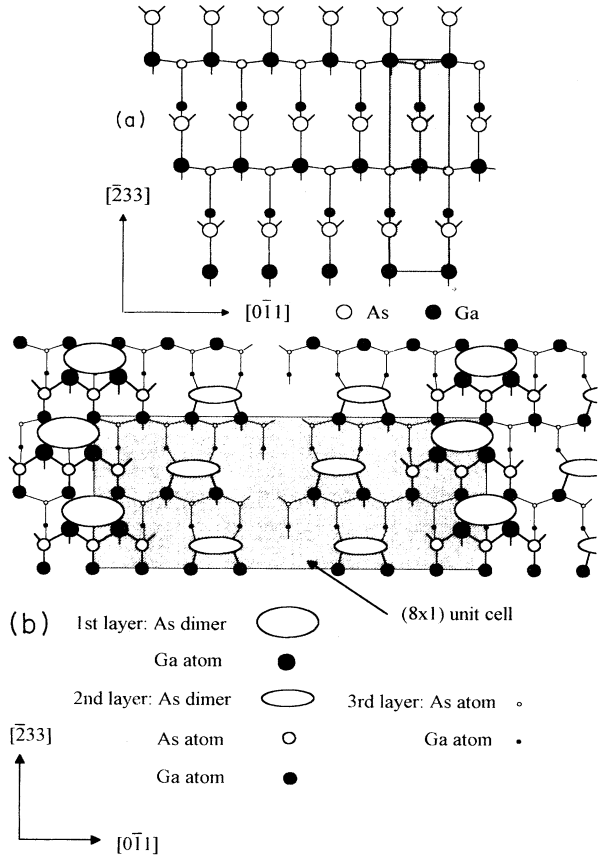

FIG. 3. Ball-and-stick model of (a) the ideal and (b) the reconstructed $(311)A$ surface. (b) The (8×1) unit cell is shown as a hatched square.

$(0.2$ nm) into the $[0\bar{1}1]$ direction. Since there are twice as many As dangling bonds than Ga dangling bonds per unit area, this surface is polar. As a qualitative measure for the surface energy and the polarity of the surface, we calculate the dangling-bond density and the excess electron density and compare these values with other ideal and reconstructed GaAs surfaces. The excess electron density is given by the difference of the number of electrons originating from the As and the Ga dangling bonds and the number of electron states below the Fermi energy, which is twice the number of As dangling bonds (spin up and down). A positive value means an excess of electrons, whereas a negative value corresponds to an excess of As dangling bonds. For nonpolar surfaces like the (110) or the (211) surface, as well as for the reconstructed surfaces this value has to vanish according to the electron-counting model. In Fig. 4, the dangling-bond density and the excess electron density are plotted for the GaAs surfaces between the (100) surface and the $(111)A$ surface as a function of the interplanar angle α. For the ideal surfaces, filled circles and solid line in Fig. 4, the dangling-bond density decreases continuously with $\cos\alpha$, and the excess electron density increases linearly with α. Also shown are the corresponding values for the reconstructed (100) (2×4) and the (111) (2×2) surfaces,[16] as well as for the $(311)A$ surface reconstruction we propose below (filled squares). The open circles show the values for the surface corrugation proposed by Nötzel *et al.*[3] The (2×2) reconstruction of the $\{111\}$ components of the $\{331\}$ facets according to an advanced model[14] has not been taken into account. The changes in the dangling-bond density and the excess electron density due to the reconstruction process are indicated by the arrows in Fig. 4. The electron-counting model requires the excess electron density to be zero. Especially interesting is that the reconstruction decreases the dangling-bond density for the (100) surface, whereas it allows an increase for the $(111)A$ surface. From this we conclude that the nonpolarity requirement outweighs the dangling-bond minimization.

The reconstruction of the $(311)A$ surface shown in Fig.

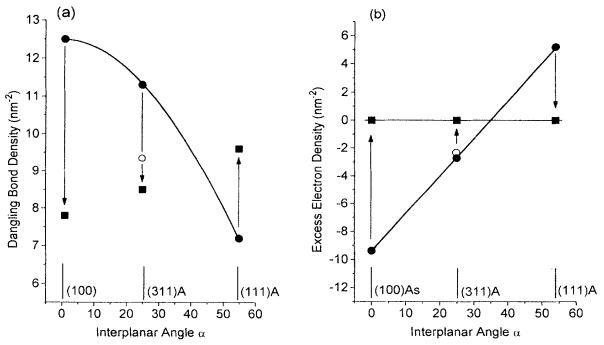

FIG. 4. Calculated (a) dangling-bond density and (b) excess electron density of the ideal (circles and line) and recontracted (squares) GaAs surfaces between the (100) surface and the $(111)A$ surface as a function of the interplanar angle α. The vertical arrows indicate the changes due to the surface reconstruction. The open circles show the values for the surface corrugation proposed by Nötzel *et al.*[3]

3(b) is constructed out of the ideal surface as follows: pairs of GaAs molecules lying eight unit cells apart in the $[0\bar{1}1]$ direction are added to the ideal surface, and one GaAs molecule is released halfway in the middle. In this way, a three-layer system as observed in the STM images is formed. A dimerization of the As atoms in the first and second layers results in a structure that is nonpolar according to the electron-counting model: within the newly formed (8×1) unit cell we find six As dimers each having two dangling bonds, all together containing six empty states. Six additional empty states are located on the eight threefold-coordinated As dangling bonds each filled with $\frac{5}{4}$ electrons. These 12 empty states are exactly filled by releasing the electrons of the 16 Ga dangling bonds. The high-resolution STM image confirms this surface structure. The zigzagging of the dimer rows along the $[\bar{2}33]$ direction, the phase shift of the corrugation along this direction between the first-layer and the second-layer dimer rows, as well as the lateral separation of the dimer rows, proves excellent agreement with the STM image. The observed As dimerization on the GaAs(311)A surface also confirms the prediction by Chadi.[12] In his calculation of the surface energy, the As dimerization was expected to reduce the surface energy very close to that of the (110) surface.

The surface corrugation according to the original model proposed by Nötzel *et al.*[3] is energetically not favored by the electron-counting model, as shown in Fig. 4. Although the dangling-bond density is decreased almost to the value of the surface reconstruction proposed in this work, the excess electron density is decreased only by 15% compared to the ideal (311) surface and does not vanish as required by the electron-counting model. The anisotropy in the optical response and the dc transport reported in Ref. 3 might also be due to the anisotropic surface roughness on the mesoscopic scale evidenced in the large-scale STM images [see Fig. 2(a)]. This surface roughness is likely to be present also at the GaAs/AlAs interface, thus, giving rise to an anisotropy in the exciton confinement and the interface roughness scattering. A redshift of the photoluminescence due to a 3.2-nm periodic corrugation of the quantum wells is not expected according to Ref. 17 and may also be attributed to the mesoscopic scale surface roughness.

In conclusion, we have investigated the (311)A surface of GaAs with STM and RHEED. The experimentally observed surface reconstruction can be explained by a model, that has successfully described also the surface reconstructions on the (100) and the (111) surfaces. The excellent agreement between the model, the high-resolution STM images, and the RHEED measurements confirms this notion. From our experimental finding, we expect the the electron-counting model can be generalized also other GaAs surface orientations. The reconstruction via As dimerization involves three atomic surface layers resulting in a vertical corrugation of only 0.34 nm in contrast to the previously proposed 1.02 nm.[3] The reported anisotropy in the optical resonance and the dc transport as well as the exciton confinement that was linked to the formation of quantum wires[3] may also be explained by the anisotropic surface roughness on the mesoscopic scale observed by STM in this work.

The collaboration between the Paul-Drude Institute and the University of Michigan has been made possible by funding from the Deutsche Forschungsgesellschaft, which is gratefully acknowledged. We want to thank Jörg Behrend and Oliver Brandt for valuable discussions. The work performed at the University of Michigan was supported by Grant No. N00014-89-J-1519.

*Present address: The Blackett Laboratory, Imperial College, Prince Consort Road, London SW7 2BZ, United Kingdom.

[1]For a recent review, see, *New Concepts for Low-Dimensional Electronic Systems,* edited by G. Bauer, H. Heinrich, and F. Kuchar (Springer, Berlin, 1992).

[2]M. S. Miller, H. Weman, C. E. Pryor, M. Krishnamurthy, P. M. Petroff, H. Kroemer, and J. L. Merz, Phys. Rev. Lett. **68**, 3464 (1992); H. L. Störmer, L. N. Pfeiffer, K. W. Baldwin, K. W. West, and J. Spector, Appl. Phys. Lett. **58**, 726 (1991); E. Kapon, D. Hwang, and R. Bhat, Phys. Rev. Lett. **63**, 430 (1989).

[3]R. Nötzel, N. N. Ledentsov, L. Däweritz, M. Hohenstein, and K. Ploog, Phys. Rev. Lett. **67**, 3812 (1991); Phys. Rev. B **45**, 3507 (1992).

[4]M. D. Pashley, K. W. Haberern, W. Friday, J. M. Woodall, and P. D. Kirchner, Phys. Rev. Lett. **60**, 2176 (1988); V. Bressler-Hill, M. Wassermeier, K. Pond, R. Maboudian, G. A. D. Briggs, P. M. Petroff, and W. H. Weinberg, J. Vac. Sci. Technol. B **10**, 1881 (1992).

[5]R. M. Feenstra, J. A. Stroscio, J. Tersoff, and A. P. Fein, Phys. Rev. Lett. **58**, 1192 (1987).

[6]D. K. Biegelsen, R. D. Bringans, J. E. Northrup, and L.-E. Swartz, Phys. Lett. **65**, 452 (1990).

[7]C. Mailhiot, C. B. Duke, and D. J. Chadi, Surf. Sci. **149**, 366 (1985).

[8]W. A. Harrison, J. Vac. Sci. Technol. **16**, 1492 (1979).

[9]D. J. Chadi, J. Vac. Sci. Technol. A **5**, 834 (1987).

[10]D. J. Chadi, Phys. Rev. Lett. **52**, 1911 (1984); **57**, 102 (1986); N. Chetty and R. M. Martin, Phys. Rev. B **45**, 6089 (1992).

[11]E. Kaxiras, Y. Bar-Yam, J. D. Joannopoulos, and K. C. Pandey, Phys. Rev. Lett. **57**, 106 (1986).

[12]D. J. Chadi, J. Vac. Sci. Technol. B **3**, 1167 (1985).

[13]B. G. Orr, C. W. Snyder, and M. D. Johnson, Rev. Sci. Instrum. **62**, 1400 (1991).

[14]R. Nötzel and K. H. Ploog, Int. J. Mod. Phys. B **7**, 2743 (1993); L. Däweritz, R. Nötzel, and K. H. Ploog, SPIE Proc. **2141**, 114 (1994).

[15]M. Wassermeier, V. Bressler-Hill, R. Maboudian, K. Pond, X.-S. Wang, W. H. Weinberg, and P. M. Petroff, Surf. Sci. Lett. **278**, L147 (1992).

[16]We have chosen the 3 dimer +1 dimer vacancy structure proposed by Chadi Ref. 9 for the (100) (2×4) surface in our calculations. For the (111) (2×2) surface, the (111)A and (111)B vacancy models give the same result as the (111)B adatom As trimer model.

[17]A. A. Kiselev and U. Rössler, Phys. Rev. B **50**, 14 283 (1994).

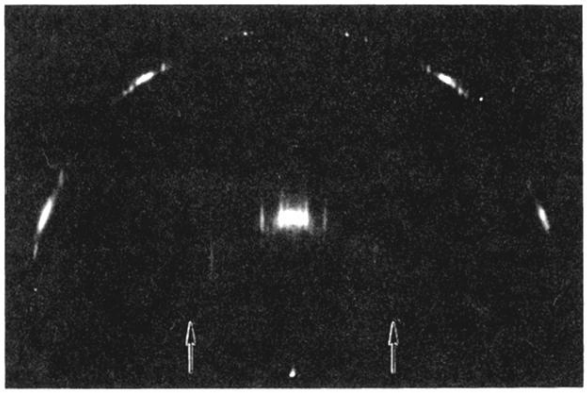

FIG. 1. RHEED pattern taken along the [$\bar{2}33$] direction with a 10-keV electron-beam energy. The position of the first-order bulk diffraction spots is indicated by the arrows.

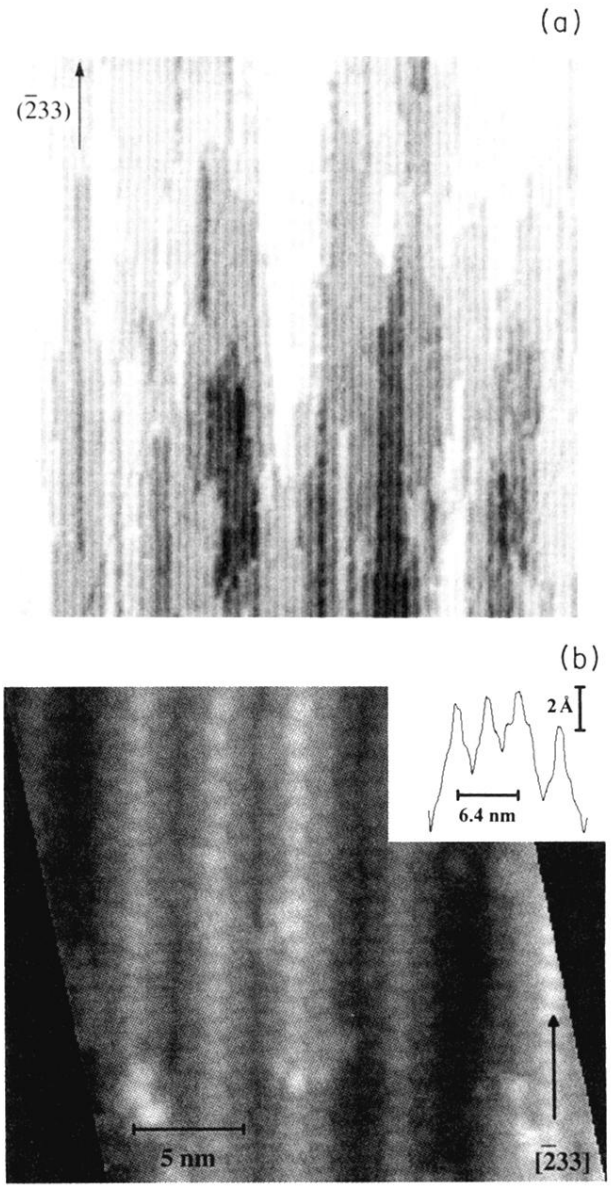

FIG. 2. STM images of the reconstructed (311)*A* surface. (a) A 200×200 nm^2 larger filled-state image showing the 3.2-nm periodicity perpendicular to the [$\bar{2}$33] direction. The surface exhibits a mesoscopic scale roughness of up to 5 ML. (b) A high-resolution empty-state image revealing the atomic structure of the reconstruction that involves the three uppermost surface layers. The linescan in the inset reveals a height modulation of the reconstruction within the same atomic layer of 0.3 ± 0.5 nm.